Cancer Management and Research

Dovepress

open access to scientific and medical research

Open Access Full Text Article

ORIGINAL RESEARCH

An expression signature model to predict lung adenocarcinoma-specific survival

This article was published in the following Dove Press journal:
Cancer Management and Research

Xiaoshun Shi,[1,2,*] Haoming Tan,[3] Xiaobing Le,[4,5,*] Haibing Xian,[6,*] Xiaoxiang Li,[1] Kailing Huang,[4,5] Viola Yingjun Luo,[4,5] Yanhui Liu,[4,5] Zhuolin Wu,[7] Haiyun Mo,[8] Allen M Chen,[4,5,*] Ying Liang,[9] Jiexia Zhang[1]

[1]National Clinical Research Center for Respiratory Disease, State Key Laboratory of Respiratory Disease, Department of Medicine, Guangzhou Institute of Respiratory Disease, Guangzhou Institute of Respiratory Health, Guangzhou 510120, China; [2]Department of Thoracic Surgery, Nanfang Hospital, Southern Medical University, Guangzhou 510515, China; [3]Department of Thoracic Surgery, Shunde Lecong Affiliated Hospital of Guangzhou Medical University, Guangdong 528315, China; [4]Mendel Genes Inc, Guangzhou 510515, China; [5]Mendel Genes Inc, Manhattan Beach, CA 90266, USA; [6]Department of Head and Neck/Thoracic Medical Oncology, The First People's Hospital of Foshan, Guangdong 528000, China; [7]Department of Biomedical Engineering, University of Minnesota, Twin Cities, MN, USA; [8]Department of Public Health, Guangzhou Medical University, Guangzhou 510000, China; [9]Department of Medical Oncology, Sun Yat-sen University Cancer Center, State Key Laboratory of Oncology in South China, Collaborative Innovation Center for Cancer Medicine, Guangzhou 510060, China

*These authors contributed equally to this work

Correspondence: Jiexia Zhang
National Clinical Research Center for Respiratory Disease, State Key Laboratory of Respiratory Disease, Department of Medicine, Guangzhou Institute of Respiratory Disease, 151 Yanjiang Road, Guangzhou 510120, Guangdong Province, People's Republic of China
Tel +86 139 0305 6432
Fax +86 20 8338 9471
Email drzjxcn@126.com

Ying Liang
Department of Medical Oncology, Sun Yat-sen University Cancer Center, State Key Laboratory of Oncology in South China, Collaborative Innovation Center for Cancer Medicine, Guangzhou 510060, China
Email wleong2014@qq.com

Background: The current TNM staging system plays a central role in lung adenocarcinoma (LUAD) prognosis. However, it may not adequately stratify the risk of tumor recurrence. With the aid of gene expression profiling, we identified 31 lncRNAs whose expressions in tumor tissues could be used as a risk indicator for the guidance of lung cancer therapy. This exploratory analysis may shed new light on identification of potential prognostic factors.

Materials and methods: A survival prediction scoring model was developed from the data that are publicly available in The Cancer Genome Atlas (TCGA) LUAD RNA Sequencing dataset. Multivariate Cox regression analysis and Kaplan–Meier analysis were performed on a cohort of 254 stage I lung carcinoma patients with survival records.

Results: Our model indicates that the panels comprising 31 lncRNAs are highly associated with overall survival (OS): 18.9% (95% CI: 10.4%–34.5%) and 89.5% (95% CI: 80.7%–99.2%) for the high- and low-risk group, respectively. The specificity and sensitivity of the model are verified, which show that the area under receiver operating characteristic curve yields 0.881, meaning our model has good accuracy and it is feasible for further applications.

Conclusion: The 31-lncRNA model might be able to predict OS in patients with LUAD with high accuracy. Its further applications in biomolecular experiments using clinical samples with independent cohorts of patients are needed to verify the results.

Keywords: lung adenocarcinoma, lncRNA, signature, survival analysis, prognosis, RNA-seq

Background

Lung adenocarcinoma (LUAD) is the most commonly occurring histological type of lung cancer, which often has major driver oncogenes such as EGFR mutation[1] and ALK fusion.[2] Previous studies have shown that the genomic alterations in LUAD are different from those in other lung cancer subtypes.[3,4] The current prediction systems for non-small-cell lung cancer (NSCLC) such as tumor, node, and metastases (TNM) staging[5] and microarray-data-based prognostic modeling[6] have not effectively distinguished lung cancer subtypes in terms of NSCLC patient survival. Moreover, the prognoses within the same TNM stage vary widely[7] and the gene signature is yet limited in coding genes[8] and microRNAs.[6,9] Evidence provides the primary rationale to develop the lncRNA model for predicting lung cancer survival.

lncRNAs are a class of RNA molecules with more than 200 nucleotides in length and have no evident open reading frames.[10] These long molecules play key roles in gene regulation and carcinogenesis including proliferation, adhesion, migration and apoptosis.[11] Current non-coding RNA profiling research reveals that lncRNAs are dysregulated among cancers[12] and some may serve as promising therapeutic

submit your manuscript | www.dovepress.com
Dovepress
http://dx.doi.org/10.2147/CMAR.S159563

targets.[13] For instance, Gutschner et al reported that elevated MALAT1 expression was associated with metastasis in multiple tumor types.[14] Previous meta-analysis showed that MALAT1 may have a role in cancer prognosis.[15] It is believed that the clinical value of lncRNA is not confined to candidate biomarkers for diagnostic and prognostic purposes. Also, lncRNA expression profiling by RNA sequencing (RNA-seq) might be useful in the classification of various cancers such as lung cancer; it is important for prognostic determinations as well.[12]

A large number of lncRNAs have been investigated in cancer research.[11,16] Some of these lncRNAs are associated with patient survival,[17,18] but most of the reports are only supported by clinical survival data from samples within a single institute[19] or pooled clinical data with some heterogeneities.[20] Given the heterogeneity of LUAD and the susceptibility of non-coding RNA decay, a panel of the lncRNA biomarkers should be more precisely stable for LUAD prognosis determinations. However, using only a single lncRNA would yield unreliable results in predicting cancer survivals. Previous studies have also observed that gene signatures and clinical characteristics among patients are associated with overall survival (OS)[21,22] aiming to overcome the limitations of the current TNM staging for predicting clinical outcomes. Several studies have reported that lncRNA expression profiles can be obtained from publicly available microarray data to perform analysis for the development of cancer survival models.[23,24] However, RNA-seq-based prognostic lncRNA expression signature for the prediction of LUAD patient survival has not yet been investigated. Though a number of prognostic lncRNA biomarkers for NSCLC have been proposed,[25–27] none of them have been successfully applied in real clinics. This is partially due to differences in the acquisition of samples and the usage of different systems for detection. In addition, the populations selected for lncRNA studies of cancer may vary and display inconsistencies. Moreover, the potential role of lncRNA as biomarkers for diagnosis and prognosis is better understood by the patterns of the lncRNA expression profile in the genome rather than as a single lncRNA expression abnormality. Notably, as we mentioned previously, the genomic characteristics of LUAD and squamous cancer distinguish greatly,[4] and previous studies identifying the signature pattern of NSCLC may be modified further by separate analysis of each cancer subtype.

To construct a reliable prognostic lncRNA signature that could improve the current staging system for predicting LUAD survival, we identified lncRNAs that can stratify the risk of LUAD recurrence through survival outcomes. RNA-seq data and corresponding clinical data were analyzed to identify lncRNAs that associate with the risk of LUAD recurrence in patients. A panel of key lncRNAs was identified by next generation sequencing technology, which could diagnose one of the major histological subtypes of lung cancer with fairly high specificity and sensitivity. We developed a risk score formula for predicting the OS time of LUAD patients. In summary, the use of the lncRNA signature provided a deeper insight into the parameters associated with LUAD than what is used exclusively for LUAD prognosis.

Materials and methods

Lung adenocarcinoma RNA-seq data from TCGA

Level 3 RNA-seq data (HTSeq-FPKM-UQ) and the corresponding clinical data of 519 LUAD patients were obtained from the public The Cancer Genome Atlas data portal website (http://cancergenome.nih.gov). Clinicopathological parameters including age, gender, smoking history and TNM stage were also assessed. Patients with incomplete clinical data or OS of less than 1 month were excluded from the analysis. No correlations between patients' gender as well as expression profile and OS were found; after data filtering and exclusions, a total of 462 LUAD samples comprising 250 females and 212 males were enrolled in the model.

Identification of differentially expressed lncRNAs in LUAD and normal lung tissue samples

To identify lncRNAs that are differentially expressed between LUAD and normal lung tissues, the raw counts of TCGA RNA-seq data (HTSeq-Counts) were downloaded for the analysis. Differential expression analysis was performed using the DESeq package in Bioconductor.[28] The thresholds for screening the expression differences of lncRNAs were adjusted p-value <0.01 and $|\log_2(\text{fold change})|>2$. The $\log_2(\text{fold change})$ indicates the fold change in the expression of each lncRNA between LUAD and normal lung tissue samples.

Cox regression analysis

First, the RNA-seq expression values of differentially expressed lncRNAs were normalized with $\log_2$ transformation. Afterward, the association between lncRNA expression and patient survival was determined by univariate Cox

regression analysis. lncRNAs with a *p*-value less than 0.05 from the univariate Cox regression analysis were used for further mining potential lncRNAs that were associated with OS time, and they were fitted in a multivariate Cox regression analysis. The mathematical model was built based on the Akaike information criterion, which allows determination of the best trade-off between the complexity of model and its goodness of fit.[29]

Risk score and survival curve

Based on the multivariate Cox regression analysis, a formula (Equation 1) was built to predict the risk score for each patient. In Equation 1, G_i represents expression value of the *i*th lncRNA and $Weight_i$ is the coefficient of each lncRNA from the Cox analysis results (Table 1). According to this risk scoring system, patients were divided into low-risk (< median risk score) and high-risk (> median risk score) groups. Subsequently, the log-rank statistical test was used to determine the differences in survivals between the low-risk and high-risk groups. A Kaplan–Meier OS curve was plotted against the two groups and the hazard ratio was calculated. Cox multivariate analysis was employed to test whether the risk score was independent of potential clinical risk factors including age, gender, smoking history and disease stage. The prognostic performance was measured by calculating the area under the receiver operating characteristic curve.

$$\text{Score} = \sum_{i=1}^{31} G_i \times Weight_i \quad (1)$$

Table 1 31-lncRNA risk score model

Ensembl ID	lncRNA	Coefficients	Univariate *p*-value	Multivariate *p*-value	References
ENSG00000249364	RP11-434D9.1	−0.2295	1.44E-06	6.48E-05	30
ENSG00000257654	RP11-497G19.2	−0.1381	3.35E-05	2.43E-05	–
ENSG00000183674	LINC00518	0.1604	4.41E-05	2.02E-05	31
ENSG00000247844	CCAT1	0.08780	5.37E-05	7.05E-03	32–34
ENSG00000238078	LINC01352	−0.1599	5.83E-05	7.40E-04	–
ENSG00000235997	AC109642.1	0.2797	8.53E-05	5.92E-02	–
ENSG00000233760	AC004947.2	0.1026	6.57E-04	1.66E-01	–
ENSG00000267123	CTD-2357A8.3	0.3168	6.98E-04	1.62E04	–
ENSG00000253227	RP11-383J24.1	−0.06522	7.17E-04	5.18E-02	–
ENSG00000268388	FENDRR	0.4477	1.08E-03	3.77E-03	35
ENSG00000237803	LINC00211	−0.07637	1.37E-03	7.11E-02	–
ENSG00000271830	RP11-1C8.7	0.08541	2.23E-03	1.84E-03	–
ENSG00000245750	DRAIC	0.13567	2.33E-03	5.98E-02	36
ENSG00000227307	RP11-95I16.2	0.08732	2.62E-03	2.00E-02	–
ENSG00000257883	RP11-497G19.1	0.07132	6.07E-03	6.61E-02	–
ENSG00000248538	RP11-10A14.5	−0.09344	7.01E-03	6.07E-02	–
ENSG00000223414	LINC00473	0.06038	8.77E-03	5.45E-02	25
ENSG00000180861	LINC01559	−0.04718	9.98E-03	1.44E-01	–
ENSG00000253288	RP11-238K6.1	−0.08147	1.04E-02	5.15E-02	–
ENSG00000270977	AC015849.16	0.2414	1.13E-02	5.58E-03	–
ENSG00000236164	RP11-268F1.3	0.05735	1.42E-02	9.19E-02	–
ENSG00000260468	LINC01290	−0.1728	1.58E-02	2.33E-03	–
ENSG00000268754	RP11-514D23.2	−0.05619	1.62E-02	8.82E-02	–
ENSG00000258474	RP11-187E13.1	−0.09878	1.82E-02	2.81E-03	–
ENSG00000241544	RP11-6F2.5	0.1623	2.01E-02	4.25E-04	–
ENSG00000236452	AC123023.1	0.04442	2.09E-02	1.32E-01	–
ENSG00000244649	CTD-2377D24.6	−0.07878	2.41E-02	1.14E-01	–
ENSG00000249241	AC195454.1	−0.1214	3.37E-02	5.00E-03	–
ENSG00000280776	LINC01202	0.1015	3.37E-02	6.94E-03	–
ENSG00000274956	UG0898H09	0.05579	4.16E-02	1.32E-01	–
ENSG00000225546	RP11-328J2.1 LVCAT5	−0.09412	4.84E-02	7.87E-03	–

Notes: The panel comprised 31 lncRNAs: RP11-434D9.1, RP11-497G19.2, LINC00518, CCAT1, LINC01352, AC109642.1, AC004947.2, CTD-2357A8.3, RP11-383J24.1, FENDRR, LINC00211, RP11-1C8.7, DRAIC, RP11-95I16.2, RP11-497G19.1, RP11-10A14.5, LINC00473, LINC01559, RP11-238K6.1, AC015849.16, RP11-268F1.3, LINC01290, RP11-514D23.2, RP11-187E13.1, RP11-6F2.5, AC123023.1, CTD-2377D24.6, AC195454.1, LINC01202, UG0898H09 and RP11-328J2.1.

Results

Differentially expressed lncRNAs in LUAD patients

The analysis of the lncRNA expression profiles in both LUAD tissues and normal lung tissues identified a total of 346 differentially expressed lncRNAs, which were used for subsequent survival analyses (Table S1). Compared to normal samples, 249 lncRNAs were overexpressed and 97 lncRNAs were underexpressed in LUAD samples. A cluster dendrogram was generated to ensure that the differentially expressed lncRNAs were good characterizations of LUAD (Figure S1).

The association of lncRNA expressions and OS time

To identify the lncRNAs associated with patient survival in LUAD, univariate Cox regression analysis for the differentially expressed lncRNAs data was assessed. With the significance level threshold of 0.05, a set of 60 lncRNAs was selected (Table S2). These lncRNAs were used in stepwise multivariate Cox regression analysis and 31 lncRNAs were chosen. A cluster dendrogram for these 31 lncRNAs is shown in Figure 1. We conducted a risk score analysis using Equation 1 on the 31 lncRNAs to calculate risk scores for patients. The coefficients of the 31-lncRNA model for determining risk scores are listed in Table 1.

Stage prognostic classifiers

Tumor stage classification was significantly associated with OS of LUAD patients. In order to test whether the 31-lncRNA model is applicable for the prediction of LUAD survival in all stages, we calculated the risk scores for patients in all stages and divided the patients into high-risk and low-risk groups according to the median risk score of patients in all stages (value=1.111). Kaplan–Meier survival curves are displayed in Figure 2, showing that the 31-lncRNA model performs well for LUAD in all stages (p-value=8.508e-11).

Survival times of low-risk and high-risk groups in stage I

Since tumor stage serves as an important factor that independently affects the survival of LUAD patients, we applied the 31-lncRNA model to stage I patients in order to test the effectiveness of the survival prediction. We divided the patients into high-risk and low-risk groups using the median risk score value 1.111, and found that the high-risk group correlated with poor prognoses for OS (log-rank test p-value 8.917e-13). Five-year OS was 18.9% (95% CI: 10.4%–34.5%) and

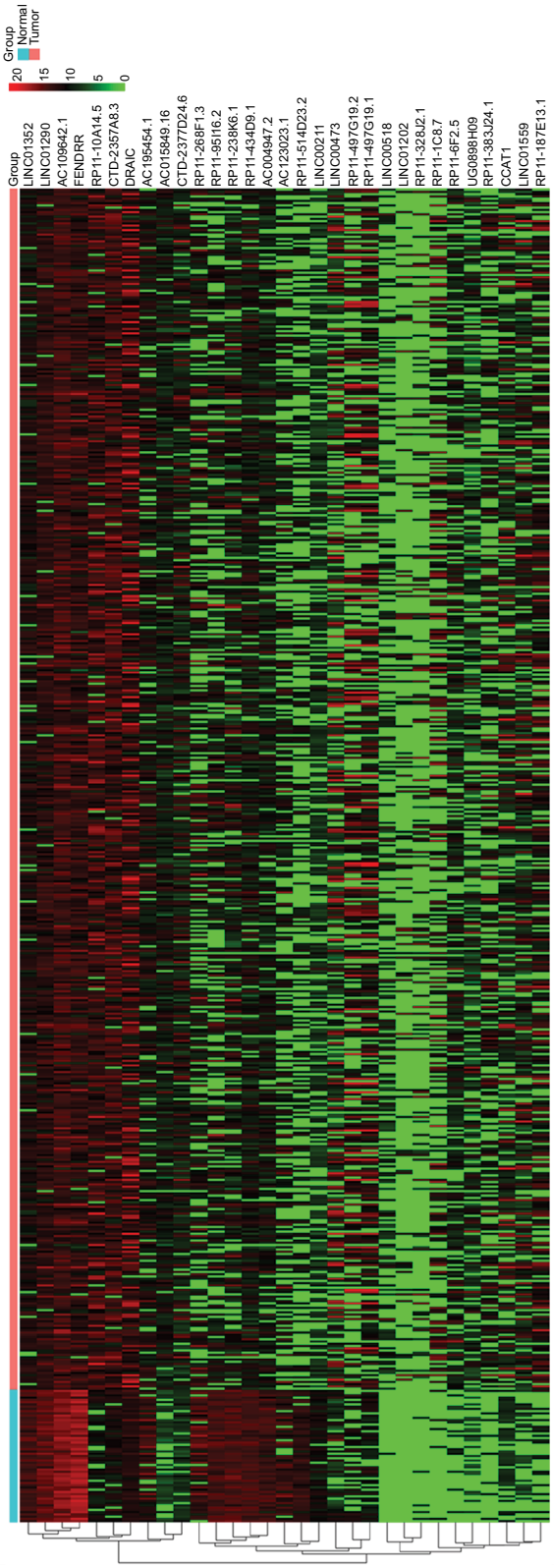

Figure 1 Hierarchical cluster dendrogram of selected 31 lncRNAs from TCGA LUAD RNA-seq dataset. The left vertical axis shows clusters of lncRNAs. The red rectangular strip in the upper portion of the picture represents normal tissue samples, and the light blue rectangular strip denotes LUAD samples. Red rectangles represent overexpressed genes, and green rectangles represent under-expressed lncRNAs. Black rectangles represent median-expressed lncRNAs.
Abbreviations: TCGA, The Cancer Genome Atlas; LUAD, lung adenocarcinoma; RNA-seq, RNA sequencing.

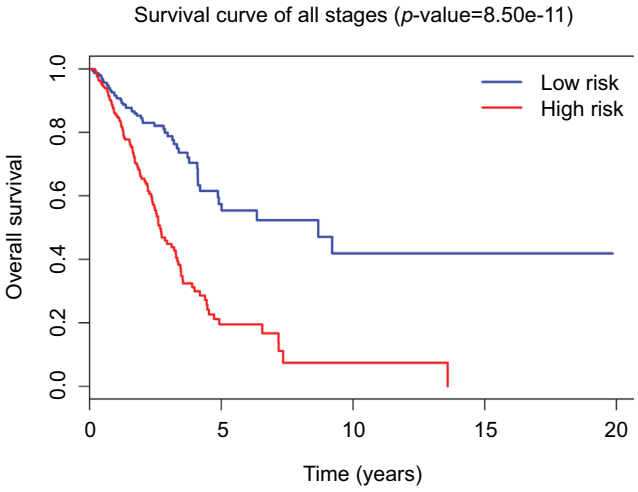

Figure 2 Survival curves for LUAD patients in all stages using 31-lncRNA model. The differences between the high-risk (n=222) and low-risk (n=240) groups were determined by the log-rank test.
Abbreviation: LUAD, lung adenocarcinoma.

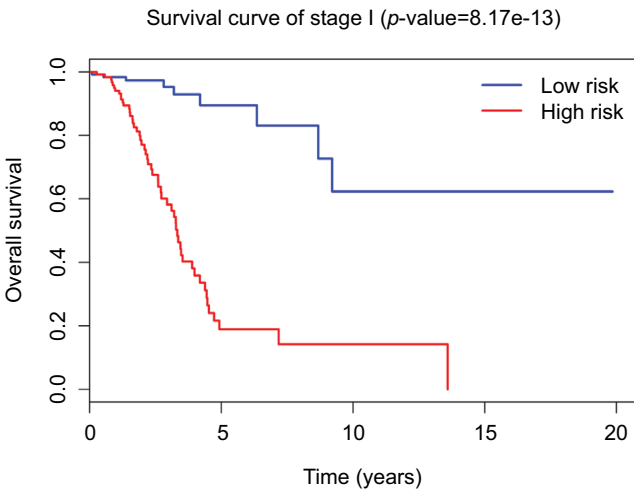

Figure 3 Survival curves for stage I LUAD patients through the 31-lncRNA model. The differences between the high-risk (n=126) and low-risk (n=126) groups were determined by the log-rank test.
Abbreviation: LUAD, lung adenocarcinoma.

89.5% (95% CI: 80.7%–99.2%) for the high-risk and low-risk groups, respectively. The Kaplan–Meier OS curves as well as ROC curves (Figure 3) indicated that the AUC of the 31-lncRNA model was 0.881 (Figure 4), which demonstrated that the 31-lncRNA model has high specificity and sensitivity in predicting the OS time of LUAD patients.[37]

Discussion

In present study, lncRNA expression data and clinical data were obtained from the public TCGA database (HTSeq-FPKM-UQ) of LUAD level 3 RNA-seq. A total of 254 stage I LUAD patients were included. lncRNAs

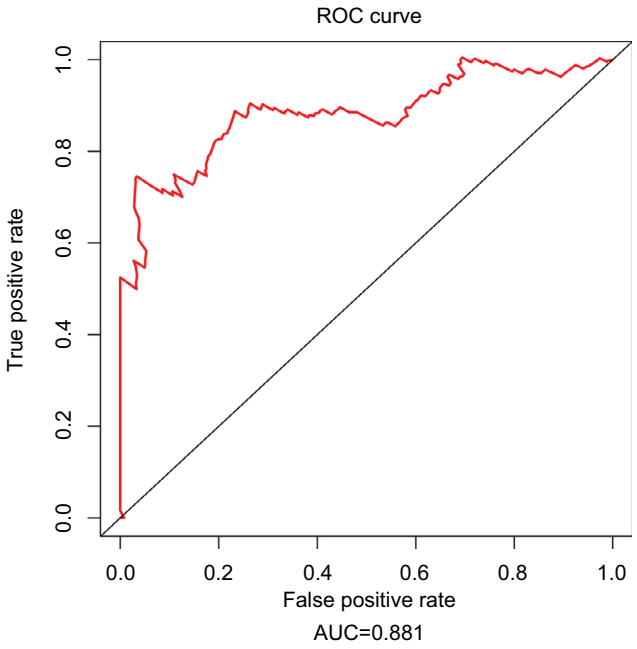

Figure 4 ROC analysis of the 31-lncRNA model. AUC of the 31-lncRNA model was 0.881.
Abbreviations: ROC, receiver operating characteristic; AUC, area under the ROC curve.

associated with survival were identified by stepwise multivariate Cox regression analysis. Subsequently, an expression pattern of 31 lncRNAs was found to be significantly associated with OS of LUAD patients. The 31-lncRNA panel accurately predicted OS and was applied to conduct a risk score analysis for further investigation of the specificity and sensitivity. ROC analysis results indicate that the statistical power of 31-lncRNA model for high-risk and low-risk patients is formidable. Therefore, the 31-lncRNA signature predicts OS fairly well based on TCGA data sets, which shows its good predictive performance. The AUC was 0.881, which is better than previously reported results.

Some of the lncRNAs that are predicted in our analysis were shown previously to function as potential biomarkers. LINC00473 has been found to correlate with poor NSCLC prognosis.[25] Its overexpression is required for the growth and survival of LKB1-inactivated NSCLC cells through CREB-regulated transcription coactivator/CREB-mediated transcription.[25] In addition, four lncRNAs including RP11-434D9.1 were found to be differentially expressed in microarray analyses.[30] RP11-434D9.1 is correlated with TNBC occurrence, and is a potential biomarker for diagnosis for breast cancer treatment.[30] Notably, one lncRNA, CCAT1, was reported to be associated with a variety of solid tumors. Abnormal expression of CCAT1 has been shown in a variety of tumors including

lung cancers.[34] Abnormally expressed CCAT1 can promote proliferation, migration and invasion in hepatocellular cells,[32] gastric carcinoma cells[38] and colon cancer cells.[39] Currently, some evidences show that CCAT1 acts as a driver lncRNA of malignancy through miRNA sponging. CCAT1 also functions as a molecular sponge for let-7c in docetaxel-resistant LUAD cells,[33] and miR-155 in acute myeloid leukemia HL-60 cells. Therefore, CCAT1 may hold an important role in the carcinogenesis of LUAD. Our lncRNA model includes cancer-associated lncRNAs that provide reference values for investigators and give eventuality of explorations in this perspective.

The risk score of the 31-lncRNA signature model was found to have an independent correlation with OS (p-value <0.001) (Table 1). Moreover, we found that one of the clinicopathological parameters of LUAD in the TCGA data, i.e., tumor staging, was significantly associated with OS,[5] which was consistent in clinical practice. Furthermore, tumor staging does not efficiently stratify the risk of early stage (stage I and II) LUAD patients. Since this parameter may affect the predictive performance of the model for cancer survival, we further tested the model in stage I LUAD patients. We calculated the risk score for each early stage patient, and the results indicate that the 31-lncRNA signature model is potentially a prognostic classifier for early stage LUAD patients (p-value <0.001). This suggests that patients in stage I and II could be divided into high-risk and low-risk groups by their lncRNA signatures. The results imply that patients with LUAD may benefit from this prognostic signature model, which could determine timeline of adjuvant chemotherapy treatments. There is a speculation that further treatments such as adjuvant therapy will alter the effectiveness of the predictions; however, relevant modifications could be adapted accordingly under the proposed framework.

Using the updated TCGA data (June 2016 version), we were able to obtain 60,483 data points including both protein coding and non-coding genes. Many of these genes are known biomarkers and some are novel genes with survival records. This broadens our scope in gene signature modeling for cancer survival prediction. The prognostic power of the signature model in this study is applied for predicting OS of stage I patients. Moreover, since these lncRNAs might have a predicative role in the outcome of LUAD, further experimental studies to survey the biological roles of these lncRNAs in carcinogenesis are worthwhile to shed new light on specific investigations. Present results show that the current prognostic model is promising and further validations on independent datasets are still needed. In addition, co-regulatory relationship between these 31 lncRNAs will affect the model efficacy, which would be validated furthermore. Based on this work, further analysis such as expression network and co-expression analysis could be applied.

This model is not without limitations. First of all, the data that we could access and analyze are still limited. The TCGA data involved fresh frozen samples, which were collected from top-notch institutions with robust tissue collection systems in place. Thus, only samples that were found to be of very high quality were included. Data in an average setting are expected to be applied by the model to further verify its robustness. For instance, further available data could be applied to analyze the correlation between the lncRNA profile and etiology such as smoking by patients or air pollutant profile of the local area of Guangzhou as well as the expression pattern. With more relevant data, a complete co-expression network could be derived.

Conclusion

In this study, we developed a signature model (Table 1) that is associated with OS in LUAD patients. Patients with a high-risk score from the model have shorter survival time, and this lncRNA panel could help to serve as a prognostic classifier for LUAD. The results of this study suggest that these lncRNAs may play specific roles in the carcinogenesis of LUAD and be of potential prognostic values. Further experiments are needed to verify the connection of 31 lncRNAs to cell survival and apoptosis linking with DNA repair. This model is LUAD specific, and proper adjustments could be made for reference of other disease-associated models.

Availability of data and material

All data generated or analyzed during this study are enclosed in this article and the supplementary information files.

Acknowledgments

This work was supported by Science and Technology Planning Project of Guangdong Province, China (411234349027) , Science and Technology Program of Guangzhou (201803010024) and the Open Project Program of the State Key Laboratory of Respiratory Disease (2014SKLRD-O09). Authors would like to extend their sincere gratitude to Mark Deiparine for editing the manuscript. They also appreciate reviewers' comments, which helped to improve this presentation. The abstract of this paper and part of the work were presented as a poster in the American Thoracic Society 2017 International Conference in Washington, DC on May 19, 2017 – May 24, 2017.

Author contributions

XL, KH, VYL, YL and AMC analyzed the TCGA data and performed the bioinformatics analysis. XS, HT, HX, XL, YL

and JZ analyzed and interpreted the patient data in the TCGA dataset and evaluated the clinical significance. JZ, YL, AMC and XS conceived and designed the study. XS, HT and HX were major contributors in writing the manuscript. All the authors read and approved the final manuscript. All authors contributed toward data analysis, drafting and revising the paper and agree to be accountable for all aspects of the work.

Disclosure

The authors report no conflicts of interest in this work.

References

1. Tsao MS, Sakurada A, Cutz JC, et al. Erlotinib in lung cancer – molecular and clinical predictors of outcome. *N Engl J Med*. 2005;353(2):133–144.
2. Solomon BJ, Mok T, Kim DW, et al. First-line crizotinib versus chemotherapy in ALK-positive lung cancer. *N Engl J Med*. 2014;371(23):2167–2177.
3. Devarakonda S, Morgensztern D, Govindan R, Genomic alterations in lung adenocarcinoma. *Lancet Oncol*. 2015;16(7):e342–e351.
4. Campbell JD, Alexandrov A, Kim J, et al. Distinct patterns of somatic genome alterations in lung adenocarcinomas and squamous cell carcinomas. *Nat Genet*. 2016;48(6):607–616.
5. Goldstraw P, Chansky K, Crowley J, et al; International Association for the Study of Lung Cancer Staging and Prognostic Factors Committee, Advisory Boards, and Participating Institutions; International Association for the Study of Lung Cancer Staging and Prognostic Factors Committee Advisory Boards and Participating Institutions. The IASLC lung cancer staging project: proposals for revision of the TNM stage groupings in the forthcoming (eighth) edition of the TNM classification for lung cancer. *J Thorac Oncol*. 2016;11(1):39–51.
6. Chen HY, Yu SL, Chen CH, et al. A five-gene signature and clinical outcome in non-small-cell lung cancer. *N Engl J Med*. 2007;356(1):11–20.
7. Chansky K, Sculier JP, Crowley JJ, Giroux D, Van Meerbeeck J, Goldstraw P; International Staging Committee and Participating Institutions. The International Association for the Study of Lung Cancer Staging Project: prognostic factors and pathologic TNM stage in surgically managed non-small cell lung cancer. *J Thorac Oncol*. 2009;4(7):792–801.
8. Kratz JR, He J, Van Den Eeden SK, et al. A practical molecular assay to predict survival in resected non-squamous, non-small-cell lung cancer: development and international validation studies. *Lancet*. 2012;379(9818):823–832.
9. Yu SL, Chen HY, Chang GC, et al. MicroRNA signature predicts survival and relapse in lung cancer. *Cancer Cell*. 2008;13(1):48–57.
10. Fatica A, Bozzoni I. Long non-coding RNAs: new players in cell differentiation and development. *Nat Rev Genet*. 2014;15(1):7–21.
11. Huarte M. The emerging role of lncRNAs in cancer. *Nat Med*. 2015;21(11):1253–1261.
12. Yan X, Hu Z, Feng Y, et al. Comprehensive genomic characterization of long non-coding RNAs across human cancers. *Cancer Cell*. 2015;28(4):529–540.
13. Mendell JT. Targeting a long noncoding RNA in breast cancer. *N Engl J Med*. 2016;374(23):2287–2289.
14. Gutschner T, Hämmerle M, Diederichs S, MALAT1 – a paradigm for long noncoding RNA function in cancer. *J Mol Med (Berl)*. 2013;91(7):791–801.
15. Shi XS, Li J, Yang RH, et al. Correlation of increased MALAT1 expression with pathological features and prognosis in cancer patients: a meta-analysis. *Genet Mol Res*. 2015;14(4):18808–18819.
16. Prensner JR, Chinnaiyan AM. The emergence of lncRNAs in cancer biology. *Cancer Discov*. 2011;1(5):391–407.
17. Ji P, Diederichs S, Wang W, et al. MALAT-1, a novel noncoding RNA, and thymosin beta4 predict metastasis and survival in early-stage non-small cell lung cancer. *Oncogene*. 2003;22(39):8031–8041.
18. Serghiou S, Kyriakopoulou A, Ioannidis JP. Long noncoding RNAs as novel predictors of survival in human cancer: a systematic review and meta-analysis. *Mol Cancer*. 2016;15(1):50.
19. Yuan JH, Yang F, Wang F, et al. A long noncoding RNA activated by TGF-β promotes the invasion-metastasis cascade in hepatocellular carcinoma. *Cancer Cell*. 2014;25(5):666–681.
20. Wei Y, Niu B. Role of MALAT1 as a prognostic factor for survival in various cancers: a systematic review of the literature with meta-analysis. *Dis Markers*. 2015;2015:164635.
21. Skrzypski M, Jassem E, Taron M, et al. Three-gene expression signature predicts survival in early-stage squamous cell carcinoma of the lung. *Clin Cancer Res*. 2008;14(15):4794–4799.
22. Raz DJ, Ray MR, Kim JY, et al. A multigene assay is prognostic of survival in patients with early-stage lung adenocarcinoma. *Clin Cancer Res*. 2008;14(17):5565–5570.
23. Zhou M, Zhao H, Wang Z, et al. Identification and validation of potential prognostic lncRNA biomarkers for predicting survival in patients with multiple myeloma. *J Exp Clin Cancer Res*. 2015;34:102.
24. Liu H, Li J, Koirala P, et al. Long non-coding RNAs as prognostic markers in human breast cancer. *Oncotarget*. 2016;7(15):20584–20596.
25. Chen Z, Li JL, Lin S, et al. cAMP/CREB-regulated LINC00473 marks LKB1-inactivated lung cancer and mediates tumor growth. *J Clin Invest*. 2016;126(6):2267–2279.
26. Han L, Zhang EB, Yin DD, et al. Low expression of long noncoding RNA PANDAR predicts a poor prognosis of non-small cell lung cancer and affects cell apoptosis by regulating Bcl-2. *Cell Death Dis*. 2015;6:e1665.
27. Schmidt LH, Spieker T, Koschmieder S, et al. The long noncoding MALAT-1 RNA indicates a poor prognosis in non-small cell lung cancer and induces migration and tumor growth. *J Thorac Oncol*. 2011;6(12):1984–1992.
28. Anders S, Huber W. Differential expression analysis for sequence count data. *Genome Biol*. 2010;11(10):R106.
29. Yamaoka K, Nakagawa T, Uno T. Application of Akaike's information criterion (AIC) in the evaluation of linear pharmacokinetic equations. *J Pharmacokinet Biopharm*. 1978;6(2):165–175.
30. Lv M, Xu P, Wu Y, et al. LncRNAs as new biomarkers to differentiate triple negative breast cancer from non-triple negative breast cancer. *Oncotarget*. 2016;7(11):13047–13059.
31. Rambow F, Job B, Petit V, et al. New functional signatures for understanding melanoma biology from tumor cell lineage-specific analysis. *Cell Rep*. 2015;13(4):840–853.
32. Zhu H, Zhou X, Chang H, et al. CCAT1 promotes hepatocellular carcinoma cell proliferation and invasion. *Int J Clin Exp Pathol*. 2015;8(5):5427–5434.
33. Chen J, Zhang K, Song H, Wang R, Chu X, Chen L. Long noncoding RNA CCAT1 acts as an oncogene and promotes chemoresistance in docetaxel-resistant lung adenocarcinoma cells. *Oncotarget*. 2016;7(38):62474–62489.
34. Xin Y, Li Z, Shen J, Chan MT, Wu WK. CCAT1: a pivotal oncogenic long non-coding RNA in human cancers. *Cell Prolif*. 2016;49(3):255–260.
35. Xu TP, Huang MD, Xia R, et al. Decreased expression of the long non-coding RNA FENDRR is associated with poor prognosis in gastric cancer and FENDRR regulates gastric cancer cell metastasis by affecting fibronectin1 expression. *J Hematol Oncol*. 2014;7:63.
36. Sakurai K, Reon BJ, Anaya J, Dutta A. The lncRNA DRAIC/PCAT29 locus constitutes a tumor-suppressive nexus. *Mol Cancer Res*. 2015;13(5):828–838.
37. Davis J, Goadrich M. The relationship between precision-recall and ROC curves. In: Proceedings of the 23rd International Conference on Machine Learning; June 25–29, 2006; Pittsburgh, PA: ACM.
38. Yang F, Xue X, Bi J, et al. Long noncoding RNA CCAT1, which could be activated by c-Myc, promotes the progression of gastric carcinoma. *J Cancer Res Clin Oncol*. 2013;139(3):437–445.
39. He X, Tan X, Wang X, et al. C-Myc-activated long noncoding RNA CCAT1 promotes colon cancer cell proliferation and invasion. *Tumour Biol*. 2014;35(12):12181–12188.

Supplementary materials

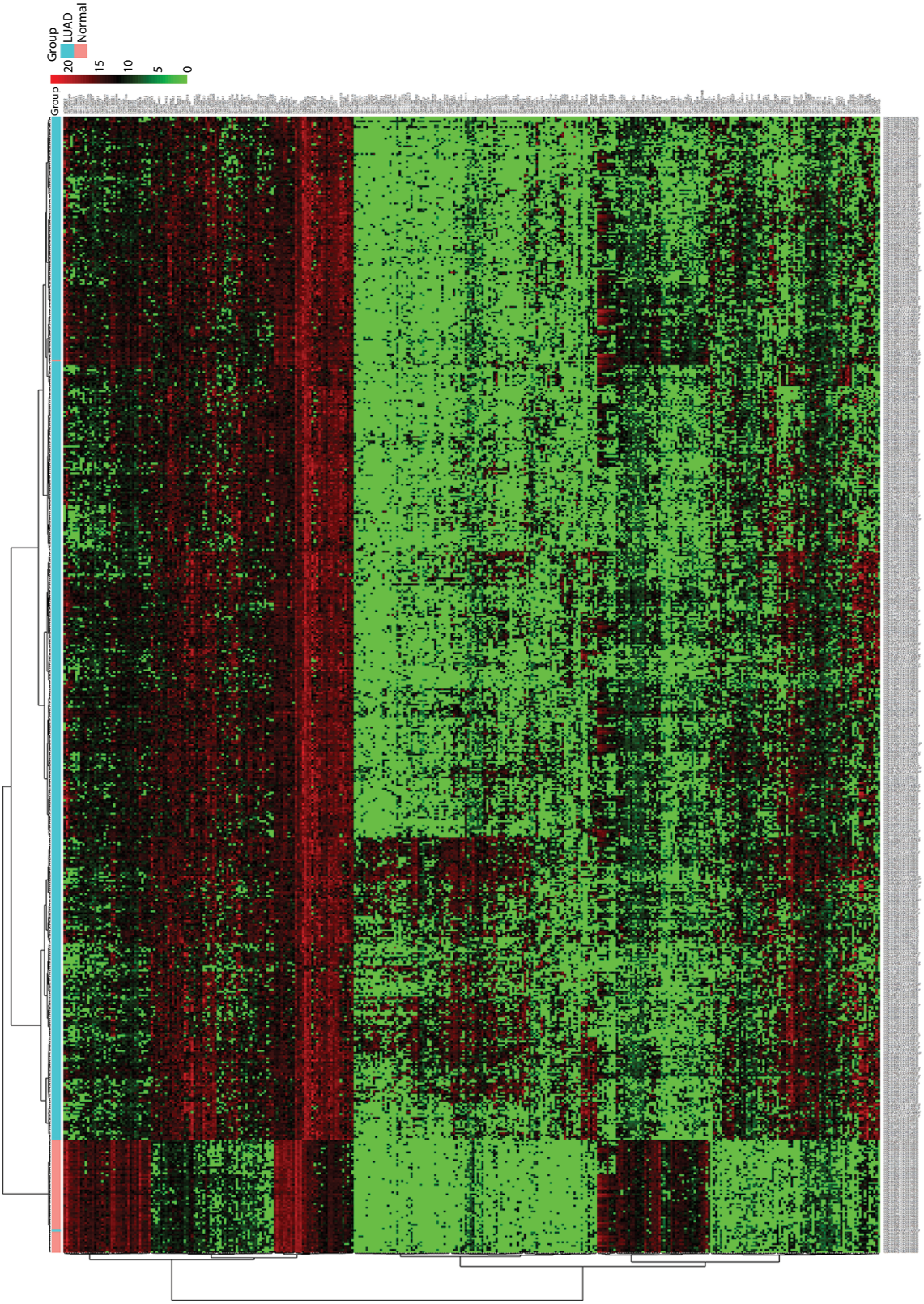

Figure S1 Hierarchical cluster dendrogram of all differentially expressed lncRNAs from TCGA LUAD RNA-seq dataset. The horizontal axis shows clusters of samples, and the left vertical axis shows clusters of lncRNAs. The red rectangular strip in the upper portion of the picture represents normal tissue samples, and the light blue rectangular strip denotes LUAD samples. Red rectangles represent overexpressed genes, and green rectangles represent underexpressed lncRNAs. Black rectangles represent median-expressed lncRNAs.
Abbreviations: TCGA, The Cancer Genome Atlas; LUAD, lung adenocarcinoma; RNA-seq, RNA sequencing.

Table S1 Differentially expressed lncRNAs

ID	Normal mean	LUAD mean	Fold change	log_2 fold change	pval	padj
FENDRR	2981.044549	202.0454063	0.067776715	−3.88306647965706	2.06E-58	2.35E-55
C14orf132	4536.086751	729.8425231	0.16089695	−2.635791116862	1.26E-36	4.41E-34
LINC01272	2806.558749	499.3803316	0.177933326	−2.49059135320854	2.22E-26	4.10E-24
RP3-340N1.2	8.089904837	537.0428035	66.38431655	6.052770537	1.41E-22	1.94E-20
RP11-88I21.2	158.625216	5.082194866	0.03203901	−4.9640266246449	1.01E-21	1.29E-19
LINC00511	137.6315305	1157.582966	8.410739614	3.072232672	4.17E-18	3.69E-16
RP11-141J13.5	193.0115915	8.868227479	0.045946606	−4.44389790523802	1.19E-17	9.84E-16
PCAT19	1231.988315	230.5331646	0.18712285	−2.41794235527104	3.12E-16	2.18E-14
FAM83H-AS1	394.577306	1902.408947	4.8213846	2.269447517	7.75E-15	4.72E-13
LINC00968	385.9077811	33.72847692	0.087400355	−3.51621705611803	3.04E-14	1.72E-12
AP002856.5	115.0495223	6.647208622	0.057776934	−4.1133625494181	1.39E-13	7.17E-12
RP11-284F21.9	6.141918547	250.6772173	40.81415527	5.350997693	1.49E-13	7.64E-12
RP1-78O14.1	574.6491884	63.41331362	0.11035135	−3.17982381789557	1.96E-13	9.89E-12
RP11-287F9.2	34.98863524	1.424814783	0.040722217	−4.6180400967434	4.68E-13	2.24E-11
GS1-600G8.5	327.0135833	29.48115008	0.090152677	−3.4714858515193	5.48E-13	2.61E-11
RP11-805I24.3	77.73713493	4.591115755	0.059059493	−4.08168722493331	7.25E-13	3.42E-11
MIR3945HG	257.2013858	21.76416665	0.084619166	−3.56287173018701	8.24E-13	3.83E-11
PVT1	109.9042973	731.3404474	6.65433896	2.734295356	1.61E-12	7.22E-11
LINC01314	581.6797822	66.86203392	0.114946464	−3.12096601344235	3.42E-12	1.48E-10
CASC9	3.877102467	177.2081692	45.70634146	5.514322439	3.74E-12	1.61E-10
LINC00665	225.0598783	1100.560291	4.890077697	2.289857388	5.82E-12	2.46E-10
LINC01082	42.576707	2.270463438	0.053326422	−4.22900566210113	9.14E-12	3.78E-10
AC011286.1	18.26333348	0.75709458	0.041454348	−4.59233276424982	1.90E-11	7.58E-10
AC128709.2	35.80940814	1.7201411	0.04803601	−4.37973985796622	3.36E-11	1.28E-09
AC109642.1	701.5189391	129.6115514	0.184758449	−2.43628775194037	4.68E-11	1.73E-09
RP11-401P9.4	736.6771455	152.074051	0.206432427	−2.27625848393677	6.33E-11	2.32E-09
RP11-89K21.1	0.764187204	80.81937877	105.758613	6.724631351	9.96E-11	3.54E-09
RP5-839B4.8	302.5155357	37.5504844	0.124127458	−3.01010581056547	3.03E-10	1.00E-08
RP11-81H3.2	0.332099875	49.41633002	148.7996044	7.217226881	6.11E-10	1.93E-08
CH17-360D5.2	501.2718126	85.9882572	0.17154018	−2.543381551426 95	2.02E-09	5.82E-08
CTD-2139B15.5	0.049962099	25.1743678	503.8692964	8.976905737	2.84E-09	7.97E-08
LINC00551	114.7444773	13.63409013	0.118821319	−3.07313438771013	6.51E-09	1.73E-07
LINC01552	42.82576179	4.110438691	0.095980515	−3.38111462894993	6.91E-09	1.83E-07
LINC00973	1.121767602	82.0215184	73.11810241	6.192156724	8.97E-09	2.31E-07
LINC00163	48.6214147	4.52837318	0.093135364	−3.42452711134183	1.79E-08	4.34E-07
CTD-2008P7.8	0.168789071	25.75784117	152.6037262	7.253646379	1.80E-08	4.35E-07
BARX1-AS1	0.200119691	30.13316326	150.5757033	7.234345187	2.10E-08	5.02E-07
AC004947.2	93.79515642	11.53895041	0.123022881	−3.02300142260912	2.19E-08	5.22E-07
LINC00656	38.02105037	3.322697759	0.087391004	−3.51637141549505	2.27E-08	5.39E-07
AC005256.1	0	11.56605236	Inf	Inf	2.37E-08	5.59E-07
AC008268.1	1184.201055	267.415188	0.225819076	−2.14676073224154	2.67E-08	6.24E-07
RP11-400N13.2	3.932808365	107.6598253	27.37479563	4.774776289	3.36E-08	7.74E-07
RP11-211G23.2	0.471898471	38.7962056	82.21303525	6.361295253	3.56E-08	8.16E-07
RP11-2N1.3	10.6461869	0.661485902	0.062133598	−4.00848257999429	3.79E-08	8.62E-07
AC098973.2	0.403399821	36.80499464	91.23701284	6.511547308	3.82E-08	8.69E-07
CTD-2527I21.15	0.884522194	55.04714502	62.23376351	5.959625589	4.17E-08	9.39E-07
CTD-3010D24.3	2.061925908	82.6561445	40.08686452	5.325057673	4.24E-08	9.50E-07
LINC00961	259.0204699	39.36654436	0.151982368	−2.718024134518 79	4.56E-08	1.02E-06
CTB-43E15.1	48.60921098	5.110697758	0.105138464	−3.24963753754913	7.42E-08	1.61E-06
MNX1-AS1	2.128585073	78.3672325	36.81658464	5.202283893	7.67E-08	1.66E-06
RP5-826L7.1	23.56576143	2.182986774	0.092633832	−3.43231700230942	9.18E-08	1.95E-06
MIR548XHG	0.05448994	13.88864612	254.8845912	7.993700349	1.35E-07	2.80E-06
CTD-2591A6.2	0.012979672	10.89487903	839.3801638	9.71318056	1.46E-07	3.00E-06
RP11-474D1.3	0.71763177	152.3136505	212.2448545	7.729585768	1.58E-07	3.20E-06

(*Continued*)

Table S1 (*Continued*)

ID	Normal mean	LUAD mean	Fold change	log_2 fold change	pval	padj
BLACAT1	32.50389347	250.1656204	7.696481673	2.944199091	1.66E-07	3.36E-06
RP11-253E3.3	516.4366306	115.9501852	0.224519676	-2.15508621	1.70E-07	3.43E-06
LINC01194	0.295282101	31.6709472	107.2565764	6.744922298	1.82E-07	3.65E-06
LINC00858	1.70453546	60.03463963	35.22052844	5.13834465	2.13E-07	4.23E-06
RP11-353N14.2	2.494260363	78.1005978	31.31212722	4.968649618	2.98E-07	5.76E-06
C11orf97	107.0602523	19.12608794	0.178647888	−2.48480923784006	3.06E-07	5.89E-06
AC011294.3	2.376383526	71.27641438	29.99364942	4.906585165	3.64E-07	6.86E-06
LUCAT1	27.88216156	254.2714042	9.119501142	3.188954908	3.68E-07	6.94E-06
LINC00942	4.510955617	430.1562509	95.35812084	6.575283901	4.14E-07	7.73E-06
LINC00491	0.434791703	26.12257311	60.08066147	5.908828791	4.25E-07	7.92E-06
RP11-209K10.2	0.053751389	11.90773641	221.5335573	7.791381441	4.73E-07	8.73E-06
RP4-594A5.1	0.09756434	13.18263545	135.1173537	7.078069168	5.00E-07	9.19E-06
XXbac-BPG27H4.8	22.54955728	1.992359195	0.088354692	−3.50054943497547	5.30E-07	9.70E-06
RP11-138J23.1	0.112415044	12.96443455	115.3265088	6.849580356	5.52E-07	1.01E-05
LINC01070	6.672623055	0.554651466	0.083123453	−3.58860061236554	8.47E-07	1.48E-05
LINC01616	11.54492084	1.208269474	0.1046581	−3.25624412826157	9.59E-07	1.66E-05
LINC01234	1.359754799	61.61418661	45.31271862	5.501844145	1.07E-06	1.84E-05
RP11-434D9.1	145.7082364	23.01730556	0.157968459	−2.66229156582695	1.24E-06	2.11E-05
LINC01518	0.049708101	10.1784877	204.7651705	7.677826531	1.25E-06	2.12E-05
RP4-666F24.3	74.67252141	13.76506789	0.184339133	−2.43956572078585	1.26E-06	2.13E-05
CTD-2021H9.3	1.267804955	45.05470345	35.53756693	5.151273006	1.49E-06	2.48E-05
RP1-27K12.2	6.617323279	334.2507059	50.51146691	5.658539035	1.63E-06	2.70E-05
DRAIC	36.17361801	498.1301911	13.77053827	3.783513048	1.68E-06	2.78E-05
RP11-776H12.1	1.356231037	42.96637185	31.68071714	4.985533088	1.82E-06	2.99E-05
CTD-2501M5.1	16.15320361	1.516648211	0.093891481	−3.41286192440999	1.83E-06	3.00E-05
RP11-109J4.1	5.028913459	92.74081613	18.44152159	4.20488579	1.89E-06	3.08E-05
AC018647.3	76.34095893	11.85510137	0.155291491	−2.68694930938768	1.92E-06	3.12E-05
AP003900.6	0	7.202839535	Inf	Inf	1.92E-06	3.12E-05
RP11-384F7.2	34.50519824	4.332125663	0.125549943	−2.99366672455614	1.96E-06	3.17E-05
LINC01214	0.231155395	18.14310901	78.48879745	6.294414851	2.01E-06	3.25E-05
LINC00702	287.9654299	60.49801789	0.21008778	−2.25093584624731	2.10E-06	3.37E-05
RP11-191L9.4	0.069368496	9.142962949	131.8028144	7.042237367	2.47E-06	3.91E-05
RP6-65G23.3	26.86213882	201.2764942	7.49294371	2.905532613	2.49E-06	3.93E-05
RP11-616M22.7	0.199187348	14.24034381	71.4922106	6.159714157	2.51E-06	3.96E-05
RP11-328J2.1	0.112184875	10.80243372	96.29135618	6.589334392	2.70E-06	4.23E-05
RP11-357H14.17	3.059063084	64.1588526	20.97336695	4.390486577	2.77E-06	4.33E-05
RP11-613D13.8	97.20655085	15.17948049	0.15615697	−2.6789311258081 2	2.78E-06	4.35E-05
RP11-403A3.3	50.55829101	6.715575788	0.132828378	−2.912364692197	3.08E-06	4.78E-05
CTD-2147F2.1	0.766586206	27.80855058	36.27582958	5.180936702	3.33E-06	5.13E-05
RP11-462G2.1	26.58592256	247.9575207	9.326647217	3.221358548	3.38E-06	5.19E-05
RP13-463N16.6	0.644364941	25.8662827	40.1422875	5.327050926	3.52E-06	5.37E-05
CTC-480C2.1	0.057369445	7.654388029	133.4227319	7.059860677	3.55E-06	5.41E-05
RP11-314N14.1	0	5.78493447	Inf	Inf	3.71E-06	5.62E-05
RP11-548L20.1	0	6.597337826	Inf	Inf	3.84E-06	5.81E-05
LINC01436	47.01255575	421.1647072	8.958557994	3.163266529	4.27E-06	6.41E-05
RP11-672A2.4	112.7122574	19.87316708	0.17631771	−2.50375070521421	4.59E-06	6.85E-05
LINC01611	0.010703432	6.26947593	585.7444548	9.194127581	4.99E-06	7.39E-05
LINC01447	19.44704841	2.442467278	0.125595783	−2.99314006562257	5.32E-06	7.85E-05
RP11-190J1.3	0.161473794	11.96958847	74.12712711	6.211929694	5.72E-06	8.39E-05
RP11-635O16.2	173.0908787	31.60001715	0.182563156	−2.45353245505645	5.93E-06	8.69E-05
RP11-312J18.6	30.12159062	3.850999272	0.12784847	−2.96749320067448	6.25E-06	9.10E-05
RP11-145G20.1	0.072000605	7.755862881	107.7194131	6.751134464	6.95E-06	0.000100215
LINC01207	39.6904527	256.7541244	6.468913983	2.693523529	7.75E-06	0.000110177
RP11-246K15.1	29.71218764	4.232615373	0.142453845	−2.81143353222706	7.79E-06	0.000110722
CTA-384D8.35	25.39251605	183.7524747	7.236481582	2.855288421	7.83E-06	0.000111175
RP11-380D23.2	0.016070831	6.540677129	406.9906047	8.66885168	7.89E-06	0.000111904
RP11-519M16.1	0	4.356779332	Inf	Inf	9.05E-06	0.000126918

(*Continued*)

Table S1 (*Continued*)

ID	Normal mean	LUAD mean	Fold change	log_2 fold change	pval	padj
RP11-497G19.1	2.853226446	81.15961497	28.44485585	4.830095865	9.55E-06	0.000133265
RP11-514D23.2	7.878561897	0.814823936	0.103422928	−3.27337204714722	9.61E-06	0.000133946
RP11-238K6.1	237.2053266	45.66999002	0.192533577	−2.3768180271936	9.99E-06	0.000138736
LINC01614	7.463214228	93.11699158	12.47679468	3.641175445	1.00E-05	0.000138953
RP11-554I8.2	3.176521931	59.72673175	18.80255608	4.232856895	1.05E-05	0.000145777
LINC00648	4.173005026	67.20016188	16.10354204	4.009306145	1.15E-05	0.000157747
RP11-962G15.1	0.020365435	5.794031604	284.5032076	8.152301108	1.38E-05	0.000186199
LINC01395	0.369343975	16.89247758	45.73643735	5.515272086	1.46E-05	0.00019587
LINC00682	0.047245583	6.04687883	127.9882349	6.999867389	1.56E-05	0.00020771
RP11-565A3.2	0.029148016	6.111575617	209.6738121	7.712002872	1.62E-05	0.000215541
RP11-78L16.1	0.017457501	4.793562405	274.5846813	8.101107332	1.63E-05	0.00021632
LINC01446	1.360809215	30.40864731	22.34600337	4.48194492	1.65E-05	0.000219192
AL163953.2	0.073783096	6.976727434	94.55726049	6.563116333	1.66E-05	0.000220138
LINC01460	3.964654475	61.87062149	15.60555198	3.963987482	1.71E-05	0.000225355
RP11-485F13.1	0.053612235	5.761779972	107.4713627	6.747808473	1.73E-05	0.000228314
RP11-25H12.1	0.034045276	5.891818201	173.0583165	7.435114463	1.75E-05	0.00022979
LINC01270	21.75472655	160.6004658	7.38232519	2.884075289	1.90E-05	0.000247566
AC008271.1	0.312509597	12.36514654	39.5672538	5.306235032	1.95E-05	0.000254239
RP11-3B12.5	0.423367868	15.97002947	37.72140184	5.237311387	2.09E-05	0.000270535
RP11-445O3.3	0.300095709	15.06287671	50.19357571	5.64943082	2.11E-05	0.000273184
AC009410.1	0.221082883	10.5770381	47.84195836	5.580204541	2.15E-05	0.000277557
RP11-308B16.2	0.090579819	8.965107915	98.9746722	6.628987479	2.20E-05	0.000283527
AC006273.4	44.09572557	7.239540695	0.164177834	−2.60666873951989	2.52E-05	0.000318512
C20orf197	15.56542845	133.8652638	8.6001657	3.104364457	2.54E-05	0.000320691
RP11-30P6.6	1.372108612	29.76532497	21.69312598	4.439166055	2.56E-05	0.00032236
RP11-100L22.1	17.15551669	2.329620109	0.135794226	−2.88050595873858	2.60E-05	0.000327024
LINC01202	0	3.184922251	Inf	Inf	2.62E-05	0.000328334
RP11-434I12.3	2.922179561	64.61721503	22.11267778	4.466801836	2.73E-05	0.000340554
RP11-203H2.2	7.481832381	0.93467043	0.124925337	−3.00086198809412	2.89E-05	0.000357659
RP1-35C21.1	24.5483517	3.848508029	0.156772564	−2.67325499584552	2.96E-05	0.000365915
AC079630.2	179.8709899	38.15962284	0.212149957	−2.23684370616534	2.99E-05	0.000368367
RP11-268F1.3	43.41104542	8.934326745	0.205807685	−2.28063124321683	3.04E-05	0.000374178
CMB9-22P13.1	46.26982154	225.8594278	4.881355068	2.287281697	3.05E-05	0.000375432
RP11-346D19.1	0.031404138	5.298279541	168.7127812	7.398425462	3.08E-05	0.000378422
GS1-120K12.4	0.023043796	4.363023917	189.3361653	7.564806198	3.10E-05	0.0003801
RP11-445O3.2	0.091370507	6.870784131	75.19695742	6.232602384	3.18E-05	0.000388637
RP11-60A8.1	0.530430449	23.10415171	43.55736321	5.444844716	3.39E-05	0.000412345
ERVMER61-1	0.028878152	6.191370585	214.3963558	7.744136574	3.50E-05	0.000424055
RP11-332J15.2	0.104232235	7.661905616	73.50802389	6.199829833	3.63E-05	0.000438331
CH17-360D5.3	157.8760522	33.98041144	0.215234743	−2.216017122935 95	3.64E-05	0.000439182
LINC00355	1.08636071	24.63118901	22.67312209	4.502911159	3.71E-05	0.000446574
RP6-114E22.1	0.524347859	17.17604946	32.75697451	5.033730208	3.80E-05	0.000456597
RP11-93K22.13	2.933986413	45.05811971	15.35730347	3.940853016	3.83E-05	0.000459654
RP11-209E8.1	0.030480874	4.184671595	137.288437	7.10106631	3.89E-05	0.000465207
LINC00844	9.717350157	1.302917952	0.13408161	−2.89881671915689	3.93E-05	0.000469451
RP11-336A10.5	0.945968126	21.9097486	23.16119117	4.533637547	4.06E-05	0.000482105
RP11-254I22.3	3.907381157	52.94771132	13.55069014	3.760294425	4.32E-05	0.000508006
RP11-474D1.4	0.024867022	6.448148137	259.3051987	8.01850732	4.34E-05	0.000510698
LINC01021	1.714172099	30.13699806	17.58108074	4.135951853	4.40E-05	0.000516859
LINC00342	268.0330582	1108.560676	4.135910262	2.048204884	4.44E-05	0.000520748
CTD-2292M14.1	0.500743025	15.89041309	31.73366833	4.987942397	4.54E-05	0.000531007
CTD-2337I7.1	1.130348765	22.54825258	19.94804903	4.318175749	5.13E-05	0.000593082
RP11-497G19.2	1.402718846	34.76559315	24.78443435	4.631362428	5.44E-05	0.000625012
RP11-95I16.2	42.54270799	7.629914892	0.179347184	−2.47917299926081	5.58E-05	0.000638325
LINC00473	21.70280685	277.1374737	12.76966043	3.674648256	6.10E-05	0.000692594
CTD-2377D24.6	3.504266369	53.82928401	15.36107086	3.941206888	6.22E-05	0.000704991
RP4-809F18.1	1.110138891	21.93340086	19.75734841	4.304317434	6.53E-05	0.000737233

(*Continued*)

Table S1 (*Continued*)

ID	Normal mean	LUAD mean	Fold change	log_2 fold change	pval	padj
AP000472.2	0	2.56134442	Inf	Inf	6.56E-05	0.000741171
RP11-10A14.5	2.677067167	63.70372646	23.79608822	4.572652527	6.72E-05	0.000756534
RP11-445O3.1	0	2.805631092	Inf	Inf	6.81E-05	0.000764257
LINC00668	2.608511281	41.40941132	15.87472963	3.988660116	6.86E-05	0.000769074
PTPRD-AS1	67.31896946	13.93071391	0.206935935	−2.27274389791362	6.89E-05	0.000770692
RP11-493L12.5	1.048265544	20.64451951	19.6939789	4.299682713	6.99E-05	0.000781026
CTA-280A3.2	0.030480874	3.650086047	119.7500441	6.903882378	7.15E-05	0.000796631
RP3-332B22.1	9.995435357	1.408349233	0.140899239	−2.82726427707433	7.25E-05	0.000805007
RP11-523L20.2	0.922996356	20.06486646	21.73883605	4.442202792	7.25E-05	0.000805007
LINC00891	55.47383928	10.10764693	0.18220565	−2.45636040110787	7.47E-05	0.000826613
RP11-734K21.5	3.644156467	50.53796856	13.86822136	3.793710865	7.64E-05	0.00084379
ELFN1-AS1	2.771164086	40.00344208	14.43560931	3.851560098	7.70E-05	0.000849695
RP11-1C8.7	0.176949315	8.41859726	47.57632019	5.572171785	7.74E-05	0.000853983
RP11-244M2.1	2.952550924	42.47322164	14.38526303	3.846519695	7.75E-05	0.000854371
AC007879.7	8.31855601	83.72841952	10.06525885	3.33131237	7.86E-05	0.000865437
RP11-98G7.1	1.028073563	21.48950318	20.90269019	4.385616725	8.14E-05	0.000893046
RP11-476K15.1	0.612377189	14.32080988	23.38560306	4.547548728	8.18E-05	0.000895623
RP11-359E19.2	4.808325503	114.6118531	23.83612612	4.575077881	8.18E-05	0.000895623
LINC01197	109.6483134	26.78646601	0.244294373	−2.03330745935022	0.000105	0.001118377
RP11-114H23.1	1.411808069	23.5925861	16.71090187	4.062717691	0.0001106	0.001170638
LINC00887	1.684211344	25.87489482	15.36321134	3.941407906	0.0001131	0.001195119
RP11-796E10.1	0.494277323	13.17681298	26.65874472	4.736536945	0.0001172	0.001232341
RP11-279F6.2	0.926647451	37.61226771	40.5896198	5.343038921	0.0001172	0.001232341
MIR137HG	0.329075044	14.12067983	42.9102118	5.423249117	0.0001229	0.001284286
DGCR9	10.86895454	88.0817823	8.10397927	3.018630484	0.0001265	0.001318527
RP11-424M24.5	47.20627508	11.60340161	0.245802101	−2.02443084626143	0.0001268	0.001320354
RP11-390F4.3	12.96510823	99.27440256	7.657043876	2.936787524	0.000127	0.00132143
RP11-146N18.1	0.088973047	5.196771966	58.40838453	5.868103578	0.0001298	0.001344908
RP11-672A2.1	0.659655685	15.55565357	23.58147428	4.55958211	0.000133	0.001371961
RP11-284G10.1	0.011023084	4.099597012	371.9101707	8.538810392	0.0001341	0.001380538
RP11-187E13.1	0.500161793	13.33398821	26.65934983	4.736569691	0.0001361	0.001399941
RP11-352B15.2	0.029861505	10.21504152	342.0806	8.418192479	0.0001376	0.001413585
RP11-211C9.1	1.813918817	26.77695521	14.76193695	3.883810128	0.0001393	0.001427657
RP11-555J4.3	0.008870375	3.062780751	345.2819938	8.43163129	0.0001403	0.00143714
AC124944.5	2.76265417	37.85365672	13.70191649	3.776305792	0.0001409	0.001441588
RP11-54O7.18	1.238909912	20.57030942	16.60355546	4.053420306	0.0001416	0.001448367
RP11-180C1.1	0.024637655	6.425248209	260.7897655	8.026743443	0.0001487	0.001509641
LINC00165	20.62587252	3.409873835	0.165320223	−2.59666488401555	0.0001499	0.001519883
LVCAT1	1.990197299	34.17573512	17.17203371	4.101989005	0.0001499	0.001520056
RP11-471M2.3	0.038584292	5.614654357	145.5165836	7.185039767	0.0001503	0.00152234
LINC01352	40.51600262	8.173994017	0.201747297	−2.30937874976962	0.0001523	0.001539551
RP11-863P13.4	23.30925725	4.13816717	0.177533206	−2.49383920130296	0.000153	0.001544631
LINC00857	41.88112963	202.0652172	4.824731782	2.270448742	0.0001535	0.001548835
LINC00862	2.32519339	35.15251725	15.11810476	3.918205386	0.0001567	0.00157769
TUSC8	2.153333946	31.25383176	14.51415922	3.859389097	0.0001694	0.001687829
AC025016.1	0.073167259	4.085619145	55.83944489	5.803212694	0.0001712	0.001704804
LINC00251	0	2.133431796	Inf	Inf	0.0001741	0.001731351
CTD-2118P12.1	0.211878907	7.633743531	36.02880361	5.171078841	0.0001756	0.001744244
KIF25-AS1	7.170910509	71.03404443	9.905861236	3.30828211	0.0001787	0.001772767
LINC00898	0.105176884	5.350901966	50.87526593	5.668892525	0.0001798	0.001783054
RP11-143E21.3	0.400620918	37.32182905	93.15996099	6.54163813	0.0001812	0.00179376
LINC01506	25.79441323	4.64264937	0.179986625	−2.47403839577747	0.0001826	0.001805964
RP11-794G24.1	3.262721056	38.50398412	11.80118786	3.560860178	0.0001986	0.001945935
CASC16	0.481008373	11.07725976	23.02924521	4.525395222	0.0002009	0.001965687
RP11-626P14.2	0.259369972	9.127963895	35.19283218	5.137209716	0.0002016	0.001972043
RP11-295M18.6	24.06065069	4.644559058	0.193035472	−2.37306211641369	0.0002033	0.001985625
AC009262.2	0.024840181	2.95774541	119.0710066	6.895678354	0.0002069	0.002017711

(*Continued*)

Table S1 (*Continued*)

ID	Normal mean	LUAD mean	Fold change	log_2 fold change	pval	padj
LINC00518	0.025413895	2.744409572	107.9885475	6.754734508	0.0002168	0.002099251
RP11-144A16.8	15.30588883	3.300302346	0.215623044	−2.21341672297669	0.0002182	0.002110689
LINC01456	0.073071088	4.507000233	61.67966475	5.946723019	0.0002197	0.002124018
LINC00383	0	2.926598654	Inf	Inf	0.00022	0.002125633
RP11-95M15.1	0.46144417	10.23855666	22.18807244	4.471712436	0.0002207	0.002131873
C1orf140	11.43761516	1.969073421	0.172157691	−2.53819745810598	0.0002227	0.002149694
RP11-290F5.1	20.60088338	127.4973948	6.188928526	2.629689661	0.0002292	0.002200775
AC069277.2	0.624338061	13.93588671	22.32105903	4.480333573	0.0002375	0.002272036
RP11-21B23.2	0.016587775	6.980247321	420.8067254	8.717013952	0.0002375	0.002272036
LINC01559	1.471566858	134.0844688	91.11680391	6.509645238	0.0002397	0.002291856
RP11-101E5.1	11.07495543	2.310214527	0.208598088	−2.26120216065066	0.0002429	0.002316427
LINC00460	7.019257066	133.7094509	19.0489463	4.251639291	0.0002486	0.002363681
RP11-503C24.1	0.143290076	6.142187717	42.86540897	5.421742003	0.0002507	0.002378891
RP11-395E19.6	18.51417437	4.130031461	0.223074028	−2.16440553835265	0.0002647	0.002497087
RP4-712E4.2	0	1.832404658	Inf	Inf	0.0002712	0.002553337
RP11-148B3.2	2.742117984	36.94069515	13.47159216	3.751848463	0.0002715	0.002555377
LINC00461	0.471335949	10.62833513	22.54938361	4.495016093	0.00028	0.002624991
CTD-2003C8.2	35.9359772	7.792845047	0.216853573	−2.2052068824473	0.0002844	0.002658539
AC195454.1	32.79937	8.181260027	0.24943345	−2.00327314401599	0.0002912	0.002711381
RP11-567N4.3	0.089845281	4.744798126	52.8107659	5.72276016	0.0002931	0.002725812
RP11-6N13.1	0.013946637	2.629130868	188.5136051	7.558524837	0.0002951	0.002740914
LINC00393	0.13859528	7.187028732	51.85623002	5.69644542	0.0002987	0.002765073
AC015849.16	2.032750829	26.49131832	13.03225066	3.704014352	0.0003044	0.002811206
LINC01529	0.741558903	13.50892082	18.21692217	4.187207325	0.0003159	0.002903022
LINC01348	17.07257455	108.3122373	6.344224004	2.665443711	0.0003297	0.003011971
CTD-2535I10.1	0.148792282	5.497095837	36.94476469	5.207298035	0.0003302	0.003014629
RP11-328K4.1	0.26936578	7.510002376	27.88031339	4.801174873	0.0003311	0.003020094
RP11-383J24.1	0.163289565	5.688594195	34.8374631	5.122567664	0.0003396	0.003084342
RP11-108K3.2	0.181846636	6.773460823	37.24820519	5.219099006	0.0003427	0.003108333
LINC00896	3.963317148	41.11871525	10.37482334	3.375014866	0.0003462	0.003134167
RP11-317N12.1	0.131796345	6.912860848	52.45108177	5.712900623	0.0003796	0.003400513
RP11-408B11.2	0.439728513	9.669203483	21.98903006	4.458712063	0.0003802	0.0034053
RP11-417E7.2	2.340636303	28.40210065	12.13435022	3.601024951	0.0003807	0.003407922
LINC01290	47.04868283	10.57795983	0.224830095	−2.15309293215505	0.0003867	0.003455511
RP11-54O7.1	1.913344914	22.53012401	11.77525487	3.557686381	0.0004096	0.003640254
RP11-400N13.3	1.045452457	16.36181282	15.65046092	3.968133241	0.000418	0.003705195
RP11-352D13.5	28.39297186	5.592133077	0.196954835	−2.344063264 11207	0.0004208	0.0037264
AC116035.1	9.147585872	1.47738052	0.161504963	−2.630349593 05152	0.0004295	0.003794076
CTC-548K16.1	2.189347226	24.70197994	11.28280596	3.496053996	0.0004344	0.003831131
RP11-400D2.2	0.020365435	2.275684159	111.7424769	6.804033895	0.0004451	0.003913426
LINC01624	20.75061641	4.180082234	0.201443762	−2.31155096360526	0.0004577	0.004011851
CECR7	21.77243384	125.8651887	5.780942527	2.531304729	0.0004646	0.004063224
RP11-1124B17.1	0.298591683	7.382889597	24.7257041	4.627939699	0.0004752	0.004145143
RP11-51B23.3	19.07844748	3.808167826	0.19960575	−2.324774811 25643	0.0004797	0.004179796
CTD-2619J13.13	9.403609672	72.96560891	7.759319181	2.955930073	0.0004856	0.004227606
MIR2052HG	1.000671925	13.57924572	13.57012761	3.762362382	0.0004932	0.004285216
RP11-13K12.1	4.91254931	46.22640362	9.409860482	3.234173333	0.0005003	0.004340044
RP11-496D24.2	0.259206088	7.073858107	27.29047824	4.770325772	0.0005214	0.004506692
CTD-2319I12.5	7.185532593	1.159948584	0.161428338	−2.63103423604141	0.000528	0.004557892
RP11-108K3.1	0.347376506	7.633224561	21.9739229	4.457720545	0.000529	0.004563319
LINC00501	0.545846666	26.36442895	48.3000641	5.593953199	0.0005301	0.004571455
AC145343.2	6.888660987	57.91971477	8.407978689	3.071759013	0.0005336	0.004597971
LINC01297	0.027177225	3.503684652	128.9198825	7.010330969	0.0005377	0.0046262
AC005537.2	2.33852028	29.99912536	12.82825111	3.681252594	0.0005627	0.004812372
AC092415.1	0.093888098	4.074268566	43.39494217	5.439454996	0.0005638	0.004819731
RP5-907D15.4	0.935340979	14.82776773	15.85279386	3.986665215	0.0005675	0.004844316
RP11-53B5.1	1.670849423	20.07642753	12.01570127	3.586848945	0.0005847	0.004966619

(*Continued*)

Table S1 (*Continued*)

ID	Normal mean	LUAD mean	Fold change	log_2 fold change	pval	padj
CTD-2515H24.2	45.63838629	10.57623917	0.23173999	−2.10942107377229	0.0005875	0.00498714
CCAT1	1.572870578	73.35092847	46.63506936	5.543343358	0.0005892	0.004996469
RP11-1070N10.7	0.184249398	5.287016275	28.69489037	4.842721957	0.0006008	0.005081898
RP11-1611l6.2	1.259049232	20.44028363	16.23469767	4.021008613	0.0006038	0.005106069
RP11-13E5.2	0	1.439087312	Inf	Inf	0.0006096	0.005152781
LINC00032	17.36534103	3.740416473	0.215395509	−2.21493992414432	0.0006577	0.005502384
UG0898H09	1.365065545	34.28511993	25.11609794	4.650540438	0.0006577	0.005502384
RP11-114H21.2	0.024637655	2.190915573	88.92549205	6.474525147	0.0006604	0.005520144
RP11-6F2.5	0.392910987	7.818661649	19.89932047	4.314647261	0.0006674	0.005571454
RP11-57A19.2	4.448163806	39.38155881	8.853441674	3.146238395	0.000684	0.00568161
AF131215.8	25.38661152	5.40186529	0.212784021	−2.2325382760569	0.0007026	0.005814437
LINC00880	2.833116664	28.87371409	10.19150198	3.34929478	0.0007041	0.005824498
RP11-412P11.1	0.013077185	4.423395808	338.2528998	8.401958492	0.0007079	0.005852146
RP11-416l2.1	4.153941363	39.73619612	9.56590203	3.257901016	0.0007134	0.005890063
AC027119.1	0.08012286	2.92982626	36.56667113	5.192457391	0.0007356	0.006052435
CTD-2532K18.2	0.152314548	5.167119698	33.92400637	5.084234655	0.0007493	0.006147782
RP11-608O21.1	0.127340348	4.024944926	31.6077739	4.982207526	0.000751	0.0061573
LINC01208	0.159966171	5.498522965	34.37303597	5.103205377	0.0007512	0.006157921
LINC01385	0.024840181	5.014651394	201.8766007	7.657329889	0.0007582	0.006200559
RP11-335L23.5	19.40222931	3.87356707	0.199645464	−2.32448780242442	0.0007893	0.006420716
CTD-2066L21.3	0.326898931	7.468377697	22.84613679	4.513878325	0.0007941	0.006453602
RP11-527D7.1	0.34513589	7.524860534	21.80260224	4.446428432	0.0008017	0.006510187
CTD-2357A8.3	8.527054324	62.08208945	7.28060208	2.864057761	0.0008023	0.006512962
WASIR2	2.349195539	27.0198068	11.50172744	3.523778651	0.0008121	0.006572905
CTD-3224I3.3	5.761709005	1.085824557	0.188455293	−2.40770578180368	0.0008245	0.006656382
LINC00160	1.208490538	16.49896283	13.65253786	3.771097252	0.0008244	0.006656382
RP11-1070N10.5	0.379387194	8.075135874	21.28468225	4.411743648	0.0008288	0.006685208
RP11-431M3.1	0	1.27573314	Inf	Inf	0.0008302	0.006693217
RP11-439L18.1	17.5153354	3.441407064	0.196479655	−2.34754815942662	0.0008572	0.006878542
CTD-2227E11.1	7.436698946	55.33302673	7.440536068	2.895406567	0.0008596	0.006894349
AC073316.2	0.803122018	12.88094016	16.03858427	4.003474895	0.0008636	0.006922829
AP000696.2	0.122308734	3.888455795	31.79213498	4.990597998	0.0008916	0.007112504
AC113617.1	0.034273478	2.532291752	73.88487836	6.20720722	0.0008927	0.007118458
CTD-3193K9.11	16.9276694	3.646499793	0.215416529	−2.21479913946623	0.0009094	0.007223302
LINC00221	0.775103091	29.93029643	38.6146008	5.271074552	0.0009462	0.007463356
AC009236.2	0	1.201393756	Inf	Inf	0.0009577	0.00754877
RP1-15D23.2	7.518156156	1.349856565	0.179546226	−2.4775727659696	0.0009674	0.007613436
RP11-396O20.2	0.352826839	6.438018483	18.24696357	4.189584504	0.0009719	0.007642504
RP11-180l4.4	10.41379331	2.094411629	0.201118993	−2.31387876020148	0.0009838	0.007723993
RP11-44F21.5	33.20806617	153.8097204	4.6316976	2.211541064	0.0009939	0.007794766
RP11-1038A11.1	1.083883723	14.98103809	13.82162843	3.788855696	0.001023	0.007985538
CTD-2384A14.1	0.253655009	5.851179741	23.06747167	4.52778798	0.0010318	0.0080419
RP11-297L17.2	0.083741799	7.539747664	90.03565424	6.492424519	0.0010378	0.008074388
RP11-57A1.1	0.48785861	9.638518569	19.75678684	4.304276427	0.0010588	0.008208608
C2orf48	4.01442139	32.8755688	8.189366688	3.033751888	0.0010674	0.008269797
RP11-237N19.3	0.160542571	4.900646687	30.52552765	4.931944328	0.0010817	0.008358608
LINC00211	11.41344477	2.360440974	0.206812318	−2.27360597482263	0.0010823	0.008359735
LINC01224	14.4337681	83.98266477	5.818485111	2.540643585	0.0011596	0.00886389
LINC01166	10.83587471	2.029500302	0.187294552	−2.41661915813136	0.0011717	0.008935899
AE000662.93	0.339497407	6.717885015	19.78773588	4.306534643	0.0011933	0.009078381
RP11-542G1.1	0.137575742	4.005799728	29.11704973	4.863792278	0.0011958	0.009090409
RP4-712E4.1	0.164668015	4.761429414	28.91532656	4.85376249	0.0012048	0.009148073
AC123023.1	15.03746187	3.182678961	0.21165001	−2.24024753521389	0.0012052	0.009148937
LINC01169	26.07034603	5.909136381	0.226661218	−2.14139053041161	0.0012091	0.009161157
LINC01597	6.843536565	120.5297366	17.61220028	4.13850325	0.0012102	0.009165339
XX-C2158C6.3	0.19573641	4.63839754	23.69716269	4.566642427	0.0012379	0.009354967

(*Continued*)

Table S1 (*Continued*)

ID	Normal mean	LUAD mean	Fold change	log_2 fold change	pval	padj
AC012531.25	0.880731502	12.4013134	14.08069699	3.815646843	0.0012603	0.0094977
RP11-356N1.2	26.45955415	6.450364988	0.243782074	−2.03633605028418	0.0012828	0.009626315
CTA-384D8.34	6.67355633	48.20996772	7.224029488	2.852803782	0.0012911	0.009682676
RP11-815M8.1	28.95577384	129.7764163	4.481883891	2.164105274	0.0012971	0.009713388
LINC00470	3.498161861	31.80328976	9.091428876	3.184507057	0.0013214	0.009880132
RP11-414H23.3	0.120894388	5.0694786	41.93311784	5.390018197	0.0013224	0.009886058
LINC01168	8.184913316	1.497808714	0.182996283	−2.45011374980004	0.0013293	0.009929169
RP11-513G11.2	0.245711727	5.522181353	22.47422792	4.490199649	0.0013406	0.009996557

Abbreviations: LUAD, lung adenocarcinoma; pval, *p*-value; padj, adjusted *p*-value; Inf, infinity.

Table S2 Univariate Cox regression result

ID	Coefficient	HR	95% lower confidence limit	95% upper confidence limit	z-score	Pr(>|z-score|)
RP11-434D9.1	−0.0966741972375059	0.907851739	0.872852909	0.944253918	−4.81960124604818	1.44E-06
RP11-497G19.2	−0.0473439461021022	0.953759299	0.932661358	0.975334502	−4.14823078202511	3.35E-05
LINC00518	0.062426122	1.064415819	1.033004562	1.096782218	4.084624611	4.41E-05
CCAT1	0.061524925	1.063457002	1.032176397	1.095685582	4.039030045	5.37E-05
LINC01352	−0.0775259586521217	0.925403002	0.891074473	0.961054033	−4.01965107946729	5.83E-05
AC109642.1	−0.198604826848537	0.819873821	0.742542429	0.90525882	−3.92910649036593	8.53E-05
RP11-21B23.2	0.047448381	1.048592072	1.023032534	1.074790193	3.768560627	0.000164192
LINC00968	−0.112456959219412	0.893635809	0.84257779	0.947787811	−3.74643656176588	0.000179364
C20orf197	−0.100336612475274	0.90453289	0.855976172	0.955844071	−3.56415277554824	0.000365033
RP5-839B4.8	−0.0557950614001376	0.945732933	0.91625924	0.976154719	−3.45398842120303	0.000552361
AC004947.2	−0.0706775712013429	0.931762271	0.894635793	0.97042946	−3.40683866899199	0.0006572
RP11-89K21.1	0.059434635	1.061236391	1.025517262	1.098199629	3.402401772	0.000667964
CTD-2357A8.3	0.13369701	1.143046436	1.058023925	1.234901333	3.390186923	0.00069845
RP11-383J24.1	0.045436493	1.046484543	1.019296977	1.07439728	3.383076937	0.000716785
RP1-78O14.1	−0.115817984483236	0.890637318	0.831897408	0.953524828	−3.32705805740635	0.000877681
RP11-805I24.3	−0.0598564532269907	0.941899731	0.909016263	0.97597275	−3.30135693597998	0.000962184
RP11-284F21.9	0.084983399	1.088698993	1.035089542	1.145084988	3.298601424	0.000971678
FENDRR	−0.135464297017085	0.873310342	0.80517459	0.9472119	−3.26848592198045	0.001081246
CTD-2515H24.2	−0.0655750561616684	0.936528752	0.900229633	0.974291526	−3.25129345987659	0.001148812
RP11-403A3.3	−0.0570717782629788	0.94452627	0.912376211	0.977809225	−3.23000664904904	0.001237873
LINC00211	−0.0561909155082247	0.945358635	0.913378013	0.978459012	−3.20016448786522	0.001373492
RP11-297L17.2	0.043563702	1.04452653	1.015786206	1.074080023	3.060244919	0.002211561
RP11-1C8.7	0.034638156	1.035245043	1.012514154	1.05848624	3.057859117	0.002229244
LINC00857	0.248979002	1.282715098	1.093148801	1.505154671	3.051526147	0.002276812
DRAIC	−0.0800454062234564	0.923074432	0.876720986	0.971878649	−3.04508603164289	0.002326138
RP11-95I16.2	−0.0413777158115412	0.959466656	0.933951603	0.985678766	−3.00890457823107	0.002621915
RP11-290F5.1	−0.133421168696628	0.875096451	0.799664272	0.957644134	−2.90098183652288	0.003719954
AC018647.3	−0.0913680429835309	0.912681743	0.856456575	0.972598014	−2.8164183505713	0.004856238
RP11-414H23.3	0.038543325	1.039295755	1.01115299	1.068221799	2.75183347	0.005926265
RP11-497G19.1	−0.0348532420354657	0.965747137	0.942001824	0.990091005	−2.74398781440122	0.006069779
RP11-10A14.5	0.075959951	1.078919364	1.02096391	1.140164685	2.696455799	0.00700817
LINC00473	0.032940886	1.033489444	1.008340619	1.0592655	2.620796567	0.008772459
LINC01559	0.040581086	1.04141575	1.009758111	1.074065911	2.576506327	0.009980438
RP11-238K6.1	−0.0407567082381766	0.960062677	0.930609742	0.99044777	−2.56371519366881	0.010355848
RP11-244M2.1	0.088962784	1.093039977	1.020423104	1.17082452	2.536369928	0.011200834
AC015849.16	0.093847381	1.098392098	1.021472885	1.1811035	2.533511725	0.011292596
RP11-523L20.2	−0.0417082104798268	0.95914961	0.928042202	0.991299718	−2.47943393724725	0.01315911
RP11-268F1.3	−0.0325167502190428	0.968006235	0.943161443	0.99350549	−2.45111781159234	0.014241333
RP11-396O20.2	−0.0347610659147038	0.96583616	0.939171135	0.993258261	−2.43353421830656	0.014952222

(*Continued*)

Table S2 (*Continued*)

ID	Coefficient	HR	95% lower confidence limit	95% upper confidence limit	z-score	Pr(>|z-score|)
RP11-384F7.2	−0.0318829689497701	0.968619934	0.943888271	0.993999613	−2.416031735763 39	0.015690694
LINC01290	−0.0631607723769502	0.93879253	0.891844983	0.988211439	−2.413013460811 64	0.015821235
CTA-384D8.35	−0.116005976007262	0.890469902	0.810200598	0.978691756	−2.406835094723 74	0.016091434
RP11-514D23.2	−0.036318585473227	0.964333022	0.936214792	0.993295754	−2.405504371065 66	0.016150159
RP11-187E13.1	0.035238067	1.035866285	1.006007816	1.066610959	2.361351517	0.018208462
CTD-2147F2.1	0.027880691	1.028272995	1.004587271	1.052517171	2.344891972	0.019032593
RP11-57A1.1	0.047463564	1.048607994	1.007554757	1.091333962	2.32932886	0.019841651
RP11-6F2.5	0.038928927	1.039696587	1.006131811	1.074381091	2.325075242	0.020067937
AC123023.1	−0.0318790237776102	0.968623755	0.942769369	0.995187169	−2.309470456471 77	0.020917489
LINC01447	−0.0412205591656668	0.959617454	0.926335577	0.9940951	−2.288811057716 81	0.022090333
CTD-2377D24.6	0.052951369	1.054378368	1.006961856	1.104027661	2.255478779	0.024103293
CTD-2118P12.1	0.031079456	1.031567465	1.003916904	1.059979596	2.241963905	0.024963705
RP11-203H2.2	−0.0384577340761104	0.962272375	0.929902199	0.995769367	−2.202802477030 62	0.027608674
RP11-400N13.3	0.045409352	1.046456141	1.004263951	1.090420955	2.162601122	0.030571872
RP11-253E3.3	0.161337856	1.17508191	1.015145464	1.360216387	2.161336638	0.030669345
AC145343.2	−0.115899603699602	0.890564628	0.801619427	0.989378912	−2.158861039975 89	0.030860949
AC195454.1	−0.0338647123718174	0.966702279	0.936959527	0.997389181	−2.123923128623 89	0.033676572
LINC01202	0.031596135	1.032100592	1.00244083	1.062637914	2.12383203	0.033684192
UG0898H09	0.034234839	1.034827596	1.001301296	1.069476447	2.037355312	0.041614449
RP11-401P9.4	−0.0886701381246491	0.915147396	0.839321207	0.997823896	−2.009329819315 33	0.044502168
RP11-328J2.1	−0.0328048474651287	0.967727396	0.936714123	0.999767473	−1.973957372926 72	0.04838659

Abbreviations: HR, hazard ratio; Pr, probability.